Domain wall distribution and magnetoresistance of a zigzag magnetic wire

Zhi-Yong Zhang* and Shi-Jie Xiong†
Department of Physics, Nanjing University, Nanjing 210093, China
(Received 4 November 2002; published 19 March 2003)

The domain wall (DW) distribution and the resultant magnetoresistance (MR) of a zigzag ferromagnetic wire in nanometer scale are investigated. The DW structure is determined by numerically locating the minima of the total free energy and the conductance is calculated via the transfer matrix method from the obtained magnetic configurations. With the in-plane external field parallel or perpendicular to the axis of the wire, the single or multiple domain pattern is formed in the remanent structure. The DW contribution to the MR undergoes a transition from positive to negative with their thicknesses reduced and the position of the transition determines the MR behavior of a practical structure. The obtained results are consistent with the recent experiment on cobalt zigzag wires and the seemingly contradictory results of previous experiments can be explained in a unified manner from the present picture.

DOI: 10.1103/PhysRevB.67.094412 PACS number(s): 75.60.Ch, 73.63.Nm, 75.47.De, 75.75.+a

I. INTRODUCTION

The properties of ferromagnetic structures in nanometer scale have attracted a lot of interest due to the development of nanotechnology and the need in the magnetoelectronics or spintronics.[1] In a uniformly magnetized ferromagnetic metal, the magnetoresistance (MR) is produced mainly from two factors: the anisotropic MR (AMR) and the Lorentz MR.[2] The former depends on the relative orientation between the current **j** and the magnetization **M**. The later is due to the Lorentz force of the internal magnetic field $\mathbf{H}_{\text{in}}$ acting on the moving charges. However, except ferromagnetic ellipsoids in saturation, **M** is generally nonuniform. In a stable or metastable state the distribution of **M** should locate in one minimum of the free energy and the competition of the magnetostatic, magnetocrystalline and exchange energies results in the formation of domains.[3] Inside domains **M** is in a single direction, but in domain walls (DW), **M** varies rapidly, leading to the precessional behavior of electronic spins.[4] The question about how the DW's contribute to the MR is still open.[5]

The existing experimental results suggest both the positive[6–8] and negative[9,10] contributions of DW's to the MR. Gregg *et al.* found giant MR (GMR) effect in thin cobalt films and attributed it to the mechanism that the carrier scattering is corresponding to the admixture with the minority spin states and hence leads to the deviation of spin orientations from the spin quantization axis.[6] This positive MR can be explained with the same Hamiltonian used to understand the GMR of magnetic multilayers[11] in terms of the admixture of two spin channels due to spin flip scattering in the walls. The experiments on magnetic superlattices[7] and submicron ferromagnetic structures[8] supported this theory. With another approach, the negative MR was detected in the epitaxially grown Fe wires with striped domain structures.[9] In these experiments, the authors eliminated the contributions to the MR from conventional sources by choosing a compensation temperature. The negative MR was also found in cobalt zigzag wires where the domain patterns are artificially controlled by changing the direction of $\mathbf{H}_{\text{ex}}$.[10] A theoretical calculation based on the linear response theory showed that the DW's cause the decoherence of the conduction electrons that destroys the weak localization and leads to the negative MR.[12] In the meantime, van Gorkom *et al.* described a band bending effect which could justify either negative or positive MR.[13]

Up to the date a detailed theoretical treatment for the DW contribution to the MR still lacks. This treatment should include the determination of the domain patterns in the magnetization processes of a real structure from the free energy minima, by taking three competing factors, the nonuniform exchange interaction, the anisotropy, and the magnetostatic energies, into account. It should also include the calculation of the conductance from the structure with the obtained domain patterns. In this paper we present an effective method to do such calculations. This is illustrated by an calculation on a zigzag wire with nanometer scale for which the MR was investigated in a recent experiment by Taniyama *et al.*[10] In the investigation the width of the wire is much larger than its thickness, the easy axis and the external field $\mathbf{H}_{\text{ex}}$ lie in the plane formed by the zigzag structure. These characteristics suggest the two-dimensional (2D) feature and prevent us from the time-consuming 3D calculations. In the zigzag structure the domain patterns can be artificially adjusted by changing the orientation of $\mathbf{H}_{\text{ex}}$ relative to the zigzag axis.[10] This allows us to isolate the DW contribution from other factors, and consequently, there is no need to adopt the compensation temperature.[9]

Our numerical calculations demonstrate that the wide DW's produce a positive contribution to the MR, but if their thicknesses are reduced to a certain value, a transition from positive to negative occurs. We attribute this transition to the mixture among channels with different wavelengths, which is affected by the DW thicknesses relative to the wave lengths. This is a possible mechanism different from those discussed previously.[11–13] The position of this transition determines the MR behavior in a practical ferromagnetic structure. The DW thicknesses in the experiment on the cobalt zigzag wires[10] fall into the range where the DW contribution to the MR is negative. This is consistent with the experimental results. The transition is a robust behavior to the existence of disorder. The effect of disorder is only in the variation of the position of the transition. The position of the transition is different for various ferromagnetic structures, leading to dif-

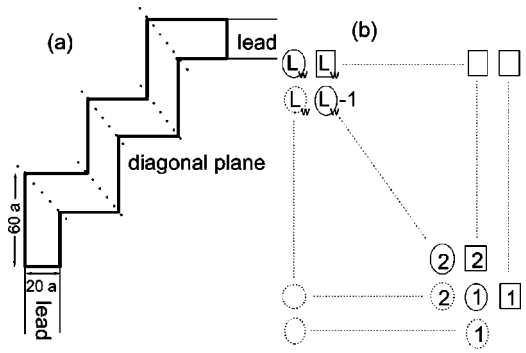

FIG. 1. Schematic illustration of (a) the wire structure in the zigzag plane and (b) the procedure of the calculation for the coefficients in the corner area.

ferent behavior of the DW contribution to the MR. From this picture the seemingly contradictory results of the previous experiments mentioned above can be explained in a unified manner.

II. MODEL AND CALCULATION TECHNIQUES

A. Determination of magnetic structure

We investigate the DW contribution to the MR in a zigzag ferromagnetic wire whose width is much larger than the thickness. Every unit with the "Γ" shape in the zigzag structure can be divided into two arms by a diagonal plane of the corner [see Fig. 1(a)]. The longitudinal directions of two successive arms are perpendicular to each other and form a 2D plane. As in the experiment,[10] we suppose that all the obtained planes for the units coincide and consequently the system is a planar one. The easy axis for the uniaxial anisotropy is assumed in the longitudinal direction in all arms of the "Γ" shaped units. The anisotropic energy in the diagonal lines of the corners is set to be zero.

The total free energy, including the nonuniform interaction, the anisotropic and magnetostatic energies, can be written as[3,14]

$$F=\int\left\{\frac{J}{2}M^2(\nabla\mathbf{m})^2-\frac{K}{2}M^2(\mathbf{m}\cdot\mathbf{e}_a)^2-M\mathbf{m}\cdot(\mathbf{H}_{\rm ex}+\mathbf{H}_{\rm in})-\left|\mathbf{H}_{\rm ex}+\mathbf{H}_{\rm in}\right|^2/(8\pi)\right\}d\mathbf{r}, \tag{1}$$

where the integration is over all space. The magnetization is denoted as $\mathbf{M}\equiv M\mathbf{m}$ with $\mathbf{m}$ being the orientation unit vector and M the magnitude which is position independent for ferromagnetic materials at temperatures low enough beneath the Curie temperature. In fact, here we only consider the situation at zero temperature. J and K are the stiff and anisotropy coefficients and they are nonzero constants everywhere except on the diagonal planes where $K=0$. $\mathbf{e}_a$ is a unit vector parallel to the easy axis. $\mathbf{H}_{\rm ex}$ and $\mathbf{H}_{\rm in}$ are the external and internal fields, respectively. $\mathbf{H}_{\rm in}$ is determined by Maxwell's equations

$$\begin{cases}\nabla\cdot(\mathbf{H}_{\rm in}/M+4\pi\mathbf{m})=0,\\ \nabla\times\mathbf{H}_{\rm in}=0,\end{cases} \tag{2}$$

where $\mathbf{H}_{\rm ex}$ is assumed to be uniform in space.

To determine the magnetic structure under an external field $\mathbf{H}_{\rm ex}$, a two-step scheme is usually taken. When we determine the free energy minima, the variation is respect to $\mathbf{m}$ with $\mathbf{H}_{\rm in}$ being specified in position. At this step the last term in the total free energy (1) can be omitted, and the integration is taken over the zigzag structure. $\mathbf{H}_{\rm in}$ is determined from the magnetic charge distribution $4\pi\nabla\cdot\mathbf{m}$ according to the Maxwell's equations (2). This two-step procedure should be repeated until the self-consistency between $\mathbf{m}$ and $\mathbf{H}_{\rm in}$ is satisfied. But a set of coupled 3D nonlinear vectorial equations have to be solved. To reduce the calculation volume, some approximations should be taken.

When the thickness of the zigzag structure is much smaller than its width, $\mathbf{m}$ is mostly in the zigzag plane if $\mathbf{H}_{\rm ex}$ is applied in that plane also. In fact, in Ref. 10 the cobalt zigzag wire is 30 nm in thickness and 250 nm in width, and, as shown in the experiment, a considerable deviation of $\mathbf{m}$ from that plane can emerge only if $\mathbf{H}_{\rm ex}$ has a large vertical component. Here we only consider the case with in-plane $\mathbf{H}_{\rm ex}$. Thus, $\mathbf{m}$ is a planar vector. Due to the nonuniform interaction in the total free energy (1), this planar unit vector can not have a significant variation in the vertical direction in so thin a film and can be viewed as a 2D variable. As a result, $\mathbf{H}_{\rm in}$ should also be taken as a 2D planar vector to satisfy the demand of self-consistency. This is possible, because we first determine $\mathbf{m}$ from the functional minima with $\mathbf{H}_{\rm in}$ specified and at this step, $\mathbf{H}_{\rm in}$ outside the zigzag structure is irrelevant.

Consequently, the minima of the free energy are determined by

$$J\nabla^2\theta+\frac{K}{2}\sin[2(\alpha-\theta)]+\frac{H_{\rm ex}}{M}\sin(\beta_{\rm ex}-\theta)+\frac{H_{\rm in}}{M}\sin(\beta_{\rm in}-\theta)=0, \tag{3}$$

where $\nabla^2=\partial_x^2+\partial_y^2$, θ, α, $\beta_{\rm ex}$ and $\beta_{\rm in}$ are the azimuthal angles of the planar polar coordinates of $\mathbf{m}$, $\mathbf{e}_a$, $\mathbf{H}_{\rm ex}$ and $\mathbf{H}_{\rm in}$, $H_{\rm ex}$, and $H_{\rm in}$ are the magnitudes of $\mathbf{H}_{\rm ex}$ and $\mathbf{H}_{\rm in}$, respectively. This nonlinear equation can also be viewed as that for the steady state solutions of the Landau-Lifshitz-Gilbert equation.[15] The boundary condition is expressed as $\nabla\theta\cdot\mathbf{n}=0$ where the unit vector $\mathbf{n}$ is in the structure plane and normal to the boundary of the zigzag structure. On the other hand, because $\mathbf{H}_{\rm in}$ is a rotationless field, it is the gradient of a scalar potential $\mathbf{H}_{\rm in}=-\nabla\Phi$, where $\nabla=(\partial_x,\partial_y)$. The magnetic charge distribution can be related to this potential by a Poisson equation $\nabla^2\Phi/M=4\pi\nabla\cdot\mathbf{m}$. With the help of the Green's function $G(\mathbf{r}-\mathbf{r}')=-(1/2\pi)\ln(1/|\mathbf{r}-\mathbf{r}'|)$, $\Phi/M=-2\int\nabla'\cdot\mathbf{m}(\mathbf{r}')\ln(1/|\mathbf{r}-\mathbf{r}'|)d\mathbf{r}'$, where $\mathbf{r}=(x,y)$, $\nabla'=(\partial_{x'},\partial_{y'})$, and $d\mathbf{r}'=dx'dy'$. Then

$$\frac{\mathbf{H}_{\rm in}}{M} = -2 \oint \frac{\mathbf{r}-\mathbf{r}'}{|\mathbf{r}-\mathbf{r}'|^2}\mathbf{m}(\mathbf{r}')\cdot d\mathbf{s}' + 2\int \mathbf{m}(\mathbf{r}')\cdot\nabla'\frac{\mathbf{r}-\mathbf{r}'}{|\mathbf{r}-\mathbf{r}'|^2}d\mathbf{r}'. \quad (4)$$

For a 2D system of planar vectors, the surface integration is just a loop integration along the boundary, where the direction of $d\mathbf{s}'$ is parallel to $\mathbf{n}$ and outward.

To solve the coupled equations (3) and (4), we adopt the following self-consistent scheme: First Eq. (3) for $\mathbf{m}$ is solved by the Newton iteration method from an initial field $\mathbf{H}_{\rm in}$, then, the obtained $\mathbf{m}$ is substituted into the Eq. (4) to yield the corrected $\mathbf{H}_{\rm in}$. These two steps are repeated until the difference between the values of $\mathbf{m}$ obtained from two successive iterations are globally less than a given tolerance of error $|\mathbf{m}-\mathbf{m}'|_{\max} \leqslant e_{\rm err}$. We start the calculation from a strong enough external field $\mathbf{H}_{\rm ex}$ for which a uniform $\mathbf{m}$ along the direction of field can be used as the initial value of the iteration. Then $\mathbf{H}_{\rm ex}$ is reduced step by step with a small enough interval, and the $\mathbf{H}_{\rm in}$ and $\mathbf{m}$ obtained in one calculation are used as the initial values in the subsequent calculation for the changed $\mathbf{H}_{\rm ex}$. This procedure ensures quick convergence of the iteration. It can be continued until a global magnetization reversal happens, which corresponds to an unstable point of the magnetization.

In this calculation, a finite difference treatment is taken with a being the difference units. Then the width of the wire can be denoted as $L_w a$ with L_w an integer. (Note that $\mathbf{m}$, $\mathbf{H}_{\rm in}$, and $\mathbf{e}_a$ are all position dependent and K is a constant except at the diagonal lines where $K=0$.) Equation (3) becomes a set of coupled nonlinear equations

$$f_{i,j} = \frac{J}{a^2}(\theta_{i-1,j}+\theta_{i+1,j}+\theta_{i,j-1}+\theta_{i,j+1}-4\theta_{i,j}) + \frac{K}{2}\sin[2(\alpha_{i,j}-\theta_{i,j})] + \frac{H_{\rm ex}}{M}\sin(\beta_{\rm ex}-\theta_{i,j}) + \frac{H_{\rm in}}{M}\sin(\beta_{{\rm in};i,j}-\theta_{i,j}) = 0, \quad (5)$$

where (i,j) are the site index of the difference lattice. When we use the Newton iteration method to solve them, we will meet a linear equation set, which can be written as

$$\sum_{i'j'} \left.\frac{\partial f_{i,j}}{\partial \theta_{i'j'}}\right|_{\{\theta_{i,j}^{(0)}\}} \Delta\theta_{i'j'} = -f_{i,j}|_{\{\theta_{i,j}^{(0)}\}}, \quad (6)$$

where $\{\theta_{i,j}^{(0)}\}$ means the set of $\theta_{i,j}$ in the last iteration. Because the corresponding matrix of this linear equation set is large and sparse, we use the Lanczos method to solve it and obtain the new set of $\theta_{i,j}$, which are $\theta_{i,j}^{(1)} = \theta_{i,j}^{(0)} + \Delta\theta_{i,j}$. On the other hand, on the difference lattice, the integrations in Eq. (4) reduce to two sums of integrations on segments, linear and areal, respectively, in each of which $\mathbf{m}$ is assumed uniform and can be moved out of the integration sign. (Of course, its vectorial character should be taken into account.) Here we have to suppose the corners of the "Γ" shape are smooth, otherwise the integral is divergent. In our numerical calculation, we simply take a truncation to guarantee the integral convergence at the corners and suppose $H_{\rm in}/M \leqslant 10^5$ at the corners.

B. Calculation of the zero temperature conductance

After obtaining the pattern of the magnetization, the electronic properties in the zigzag structure can be described by taking $\mathbf{M}$ as an effective field for the electrons[4,16,12]

$$H = t\sum_{\langle(i,j),(i',j')\rangle;\delta}(c_{i,j;\delta}^{\dagger}c_{i',j';\delta}+c_{i',j';\delta}^{\dagger}c_{i,j;\delta}) + UMha^2\sum_{i,j;\delta,\delta'}\mathbf{m}_{i,j}\cdot(c_{i,j;\delta}^{\dagger}\hat{\boldsymbol{\sigma}}_{\delta,\delta'}c_{i,j;\delta'}), \quad (7)$$

where $c_{i,j;\delta}$ annihilates an electron with spin δ on site (i,j) of the 2D lattice of the discretization with lattice spacing a, $\langle(i,j),(i',j')\rangle$ denotes the nearest-neighbor sites, t is the hopping integral, Mh is the magnetic moment in a unit area, $\hat{\boldsymbol{\sigma}}$ is the Pauli matrix, and U is the coupling strength between the magnetic moments and the electron spin.[12] The sites in Eq. (7) are within the zigzag structure. Because we investigate the zigzag wire with its width much larger than its thickness, in the above Hamiltonian, only one layer of lattice is considered. Including another one or two layers in the vertical direction can only slightly change the obtained values and can not change the qualitative conclusions.

One may take local spinor transformation[4,11,12] by rotating $\hat{\boldsymbol{\sigma}}$ to be parallel to $\mathbf{m}$ to obtain local spin eigenstates in the uniformly magnetized domains. In the domain walls electrons undergoes spin-flip scattering and the eigenstates are mixed by the rapidly changing local spins. This treatment is more suitable for a perturbation theory, but we would prefer a more strict method. We express a wave function of the electron as a linear combination of the basis functions

$$\Psi = \sum_{i,j;\delta} w_{i,j;\delta}c_{i,j;\delta}^{\dagger}|0\rangle, \quad (8)$$

where $|0\rangle$ denotes the vacuum. By applying the above Hamiltonian on Ψ, one gets the Schrödinger equation for coefficient $w_{i,j;\delta}$

$$t(\hat{w}_{i+1,j}+\hat{w}_{i-1,j}+\hat{w}_{i,j+1}+\hat{w}_{i,j-1}) + UMha^2\mathbf{m}_{i,j}\cdot\hat{\boldsymbol{\sigma}}\hat{w}_{i,j} = E\hat{w}_{i,j}, \quad (9)$$

where

$$\hat{w}_{i,j} \equiv \begin{pmatrix} w_{i,j;\uparrow} \\ w_{i,j;\downarrow}\end{pmatrix}$$

and

$$\mathbf{m}_{i,j}\cdot\hat{\boldsymbol{\sigma}} = \begin{pmatrix} 0 & \cos\theta_{i,j}-\imath\sin\theta_{i,j} \\ \cos\theta_{i,j}+\imath\sin\theta_{i,j} & 0\end{pmatrix}$$

with $\theta_{i,j}$ the azimuthal angle of $\mathbf{m}_{i,j}$ and $\imath=\sqrt{-1}$. Here, the z axis for the spinor representation is taken in the direction vertical to the plane, and the hard-wall boundary condition is applied in the transverse direction.

We suppose that the zigzag structure is attached to two nonmagnetic leads, which have the same width of the wire $L_w a$ and are along the longitudinal directions of the two outer segments [see Fig. 1(a)]. The Hamiltonian in the nonmagnetic leads is

$$H_L=t_0\sum_{\langle(i,j),(i',j')\rangle,\delta}(c^{\dagger}_{i,j;\delta}c_{i',j';\delta}+c^{\dagger}_{i',j';\delta}c_{i,j;\delta}), \quad (10)$$

where t_0 is the hopping integral in the leads. We also adopt the hard-wall boundary condition in the transverse direction for the leads. From the Schrödinger equations, for an electron at Fermi energy E_F one has equations for the coefficients in the leads

$$t_0[w_{j+1,\delta}(k)+w_{j-1,\delta}(k)]=[E_F-2t_0\cos(ka)]w_{j,\delta}(k) \equiv E_{\perp}w_{j,\delta}(k), \quad (11)$$

where j is the site index in the transverse direction, k is the wave vector in the longitudinal direction, and $E_{\perp}$ is the transverse part of the kinetic energy which should have $2L_w$ eigenvalues corresponding to $2L_w$ channels for the incident and outgoing plane waves, with the factor 2 coming from the spin degree of freedom in the leads. We denote the αth eigenvector of Eq. (11) with a $2L_w$-component vector $\hat{U}_{\alpha}$, which has longitudinal wave vector k_{α} satisfying $E_F-2t_0\cos(k_{\alpha}a)=E_{\perp;\alpha}$ with $E_{\perp;\alpha}$ being the corresponding eigenvalue of the transverse kinetic energy. Note that these eigenvectors are decoupled from each other within a lead and can be regarded as independent channels, but they are mixed when the electron passing through the zigzag structure. To obtain the conductance of the zigzag system, one should first calculate the $2L_w\times 2L_w$ transmission matrix $\hat{T}$ whose element $\hat{T}_{\alpha,\beta}$ is the amplitude of the wave transmitted into the αth channel in the right lead when a wave with unity amplitude is incident only from the βth channel of the left lead. If the wave is incident from all the channels in the left lead, with the amplitude in the β channel being u_{β}, the amplitude of the transmitted wave in the αth channel of the right lead v_{α} can be expressed with the transmission matrix as

$$\begin{pmatrix} v_1 \\ v_2 \\ \cdots \\ v_{2L_w} \end{pmatrix}=\hat{T}\begin{pmatrix} u_1 \\ u_2 \\ \cdots \\ u_{2L_w} \end{pmatrix} \quad (12)$$

and, vice versa,

$$\begin{pmatrix} u_1 \\ u_2 \\ \cdots \\ u_{2L_w} \end{pmatrix}=\hat{T}^{-1}\begin{pmatrix} v_1 \\ v_2 \\ \cdots \\ v_{2L_w} \end{pmatrix}. \quad (13)$$

If only the βth channel in the right lead has transmitted wave with unity amplitude and all other channels have zero amplitudes, the incident wave should come from all the channels of the left lead, with the amplitude in the αth channel being $\{\hat{T}^{-1})\}_{\alpha,\beta}$. From this we can calculate matrix $\hat{T}^{-1}$ and then get $\hat{T}$ if we can obtain the amplitudes of the incoming wave in all the channels of the left lead by setting the amplitude of the outgoing wave in one channel of the right lead to be unity and those in other channels to be zero. For the unity outgoing wave in the βth channel, the amplitudes on the sites of the right lead are known and can be expressed with the βth eigenvector of Eq. (11)

$$w_{i,j;\delta}=\{\hat{U}_{\beta}\}_{j,\delta}\exp(\imath k_{\beta}ia), \quad \text{for} \quad (i,j)\in \text{ right lead}, \quad (14)$$

where $\{\hat{U}_{\beta}\}_{j,\delta}$ is the component of eigenvector $\hat{U}_{\beta}$ corresponding to the jth site in the transverse direction and spin δ, and i is the site index in the longitudinal direction. Thus, the amplitudes of the wave function in the zigzag structure and in the left lead can be calculated from the right to the left one bar by another by using Eq. (9) iteratively. (Details are given in the next section.) The obtained amplitudes in the left lead are related to the incident and reflected waves and can be written as

$$w_{i,j;\delta}=\sum_{\alpha=1}^{2L_w}[\{\hat{T}^{-1}\}_{\alpha,\beta}\exp(\imath k_{\alpha}ia)+\hat{R}_{\alpha,\beta}\exp(-\imath k_{\alpha}ia)] \times\{\hat{U}_{\alpha}\}_{j,\delta}, \text{ for } (i,j)\in \text{ left lead}, \quad (15)$$

where $\hat{R}_{\alpha,\beta}$ is the corresponding reflection amplitude in the αth channel of the left lead.

This procedure can be written globally in the form of the transfer matrix

$$\sum_{\alpha=1}^{2L_w}\begin{pmatrix} [\{\hat{T}^{-1}\}_{\alpha,\beta}\exp(-\imath k_{\alpha}a)+\hat{R}_{\alpha,\beta}\exp(\imath k_{\alpha}a)]\hat{U}_{\alpha} \\ (\{\hat{T}^{-1}\}_{\alpha,\beta}+\hat{R}_{\alpha,\beta})\hat{U}_{\alpha} \end{pmatrix} =\hat{M}\begin{pmatrix} \hat{U}_{\beta} \\ \hat{U}_{\beta}\exp(\imath k_{\beta}a) \end{pmatrix}\equiv\begin{pmatrix} \hat{A}_{\beta} \\ \hat{B}_{\beta} \end{pmatrix}, \quad (16)$$

where $\hat{M}$ is the $4L_w\times 4L_w$ transfer matrix of the zigzag wire. For a given E_F, there may exist some channels in which the longitudinal wave vector k_{α} of the electron becomes complex. The leads are not transparent for the motion of electrons in these channels. Thus, only a set of N ($\leqslant 2L_w$) channels with real k_{α}, denoted as $\mathcal{S}$, contribute to the conductance. In our calculation, the Fermi energy E_F is set to be zero, which corresponds to the situation where the bands of the leads are half filled.

Now we describe the method of calculating the transfer matrix in the zigzag structure. For a straight segment of the zigzag wire, the sites can be divided into bars which are perpendicular to the axis of the segment. We use one of the coordinates (i,j) of the sites, say, i, as the index for the bars. Given the coefficients of the wave function in bars i and $i-1$, $(\hat{w}^{\dagger}_{i,1},\ldots,\hat{w}^{\dagger}_{i,j},\ldots,\hat{w}^{\dagger}_{i,L_w})$ and

$(\hat{w}^{\dagger}_{i-1,1}, \ldots, \hat{w}^{\dagger}_{i-1,j}, \ldots, \hat{w}^{\dagger}_{i-1,L_w})$, with $L_w a$ the width of the segment, the coefficients in bar $i+1$, $(\hat{w}^{\dagger}_{i+1,1}, \ldots, \hat{w}^{\dagger}_{i+1,j}, \ldots, \hat{w}^{\dagger}_{i+1,L_w})$, can be obtained from the Schrödinger equations. This is the basic spirit of the transfer matrix method. However, because of the existence of corners in the zigzag structure, it is difficult to write the transfer matrix $\hat{M}$ throughout the wire explicitly. To deal with this difficulty, we calculate the coefficients in bar $i+1$ from those in bars i and $i-1$ directly from the Schrödinger equations, instead of explicitly presenting the transfer matrix. Suppose that the electron wave is incoming from the left (lower) lead and outgoing to the right (upper) lead illustrated in Fig. 1(a). As described above, the calculation is started from the right lead and can be continued in the straight segment leftward without difficulty until the coefficients in the bar containing the site 1 marked by a solid circle [Fig. 1(b)] have been calculated. At this point the wire turns by 90°. The coefficient on site 2 marked by a dotted circle cannot be obtained directly because the Schödinger equation centered at site 1 with a solid circle contains the coefficients on sites 1 with circles and rectangular box and sites 2 with solid and dotted circles, but at this moment both the coefficients on sites 1 and 2 marked by dotted circles are unknown. However, the coefficients of the sites in and above the diagonal line can be obtained from the right to the left consecutively by using the Schrödinger equations. Then, the coefficient on site L_w marked by a dotted circle can be obtained from the values of two L_w sites marked by solid circle and rectangular box. So the coefficients of sites beneath the diagonal line can be calculated consecutively in the downward direction. This procedure can be applied to all the segments and corners, and finally one can obtain a transfer-matrix relation that connects the coefficients of the first two bars of the outgoing lead to those of the incident lead.

By running the above procedure for β from 1 to $2L_w$, one can obtain all the elements $\{\hat{T}^{-1}\}_{\alpha,\beta}$ from Eq. (16)

$$\{\hat{T}^{-1}\}_{\alpha,\beta} = \frac{\hat{U}^{\dagger}_{\alpha}\hat{B}_{\beta}e^{\imath k_{\alpha}a} - \hat{U}^{\dagger}_{\alpha}\hat{A}_{\beta}}{2\imath \sin(k_{\alpha}a)}. \tag{17}$$

In this derivation the orthogonality and normality of the set of the eigenvectors $\{\hat{U}_{\alpha}\}$ are used. The $2L_w \times 2L_w$ transmission matrix $\hat{T}$ is just the inverse of matrix $\hat{T}^{-1}$, and the conductance at zero temperature can be obtained from the Landauer-Büttiker formula[17]

$$G = \frac{e^2}{h} \sum_{\alpha,\beta \in \mathcal{S}} |\{\hat{T}\}_{\alpha,\beta}|^2. \tag{18}$$

The transfer-matrix method and the Landauer-Büttiker formula has been extensively used to investigate the phenomena of localization in mesoscopic systems.[18] In the present paper we adopt this method to study the effect of domain walls on the magnetoresistance in the zigzag ferromagnetic wire. The influence of the rapid variation of moment orientations on the conductance in different domain patterns is described in the Schrödinger equation (9). Other types of disorder is not included in the Hamiltonian (7), and we focus our attention on the influence of the domain wall scattering on the MR in clean samples. The possible effects of other types of disorder are discussed in the next section. Here we are only interested in the conductance at zero temperature. The difference between the Fermi levels of the two leads due to the bias voltage is very small and the density of current flowing through the wire is low. Consequently, the force acting on DW's by the electronic current can be neglected[19] and the effects caused by the current induced deviation of **m** from the equilibrium distribution, such as the band bending effect[13] and the spin wave excitation, are also neglected.

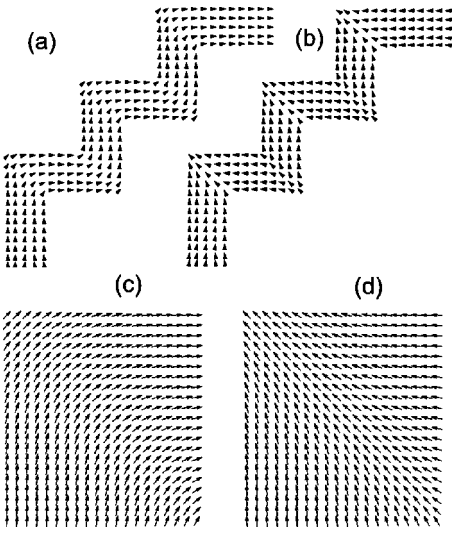

FIG. 2. Remanent domain structure of the zigzag wire in parallel (a) and perpendicular (b) external field. (c) and (d) illustrate detailed structures in the central corner of the wire for (a) and (b), respectively. Here $J/Ka^2 = 20$, $K = 100$, and $L_w = 20$.

III. RESULTS AND DISCUSSION

In Figs. 2(a) and 2(b), we plot the remanent domain structure for $\mathbf{H}_{ex}$ parallel and perpendicular to the axis of the zigzag wire. When the wire is first magnetized to saturation with a large enough parallel field, a single domain is formed in the remanent structure. On the other hand, multi-domain pattern is formed if the structure is first magnetized to saturation with a perpendicular field. In our calculations, we take $L_w = 20$ [see Fig. 1(a)]. If we plot **m** for all the sites, the magnetization can not be distinguished by eyes. Consequently, in these two figures we plot **m** on every four sites, but in Figs. 2(c) and 2(d) the detailed remanent domain structures in the central corner area are illustrated for both parallel and perpendicular cases. The obtained structures demonstrate the schematic features described in Ref. 10. Here we set $J/Ka^2 = 20$ and $K = 100$. Similar results are obtained for K not less than 20. When K is close to 20, the domain pattern is altered in the perpendicular case. This can be understood from the competition between the anisotropic and magnetostatic energies,[3] since for $K \sim 20$, $4\pi/K \sim 1$, the magnetostatic energy becomes comparable with the aniso-

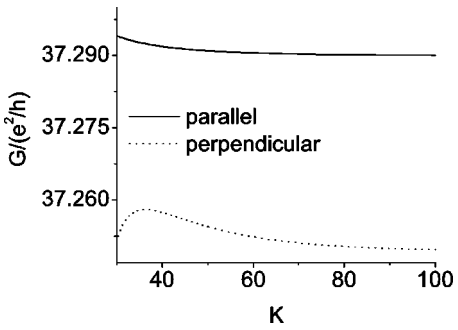

FIG. 3. The conductance as a function of K with $J/Ka^2=20$, $UMha^2/t=0.02$, $t_0/t=1$, and $E_F/t=0$ under the remanent domain structure described in Fig. 2.

tropic one and the formation of closure of domain patterns favors the reduction of the free energy. In the perpendicular case, **m** has component normal to the boundaries in the corner area of the zigzag structure, and the pattern is then more sensitive to the variation of the fraction of the anisotropic and magnetostatic energies in the free energy. In fact, even when K is near 30, some slight changes in the remanent magnetization already happen although the basic domain pattern does not alter. These changes are not easy to be detected by eyes from the figures, but their effect on the conductance is noticeable: a maxima appears at $K=36.3$ in the G-K curve of Fig. 3.

The total magnetization $\bar{M}=|\int \mathbf{M}d\mathbf{r}|$ is plotted in Fig. 4 for both the parallel and perpendicular field. The hysteresis behavior can be obviously seen. Here we focus on the range of $\mathbf{H}_{ex}$ sweeping from a positive value to the unstable point. The value of $\mathbf{H}_{ex}$ at this point represents the coercive force, that is $-0.497M$ and $-0.495M$ for the parallel and perpendicular cases, respectively. In Fig. 4 we also plot the variation of the conductance in the same magnetization process. With $\mathbf{H}_{ex}$ decreased G is reduced continuously and reaches a lowest point prior to the unstable point of magnetization for both parallel and perpendicular cases. After this point G undergoes a rapid enhancement by increasing the reversed $\mathbf{H}_{ex}$. At the unstable point where the magnetization would be reversed if a small perturbation was added, G shows a small retraction.

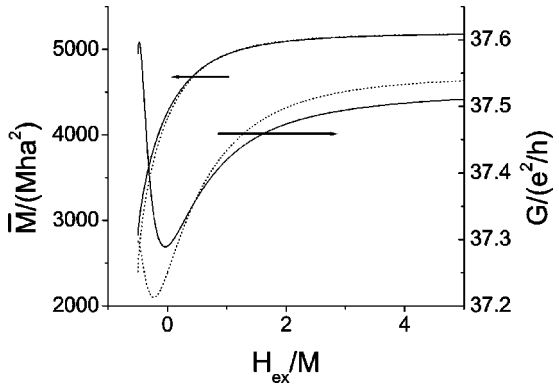

FIG. 4. The variations of $\bar{M}$ and G with parallel (solid) and perpendicular (dotted lines) $\mathbf{H}_{ex}$. Here $J/Ka^2=20$ and $K=100$. The other parameters are the same as those in Fig. 3.

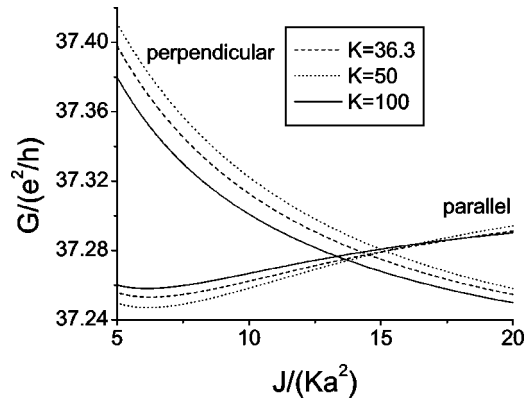

FIG. 5. The conductance as a function of J/Ka^2 in the parallel and perpendicular cases for different values of K. Other parameters are the same as those in Fig. 3.

As discussed above, the Lorentz MR effect is not important in this planar structure and is neglected in our calculation. The dependence of G on $\mathbf{H}_{ex}$ is mainly due to the mechanism of AMR. Because of the spin-orbit interaction, the local resistivity is anisotropic and determined by the angle γ between **m** and current **j** as $\rho=\rho_{\parallel}+(\rho_{\perp}-\rho_{\parallel})\sin^2\gamma$.[20] For the transport dominated by electrons with minority spin $\rho_{\parallel}>\rho_{\perp}$. With $\mathbf{H}_{ex}$ decreased, the system evolves from saturation and **m** is aligned towards the easy axis in every segment. Because the moving path of charge is along the easy axis, the local ρ increases and G decreases in this process. After passing through the zero point, $\mathbf{H}_{ex}$ drives **m** away from the easy axis, leading to the increase of G and the appearance of a minimum. The deviation of this point from the position where $\mathbf{H}_{ex}=0$ is finite, and its position depends on the system parameters J/Ka^2 and K. This deviation may come from the fact that the path of the moving charges and the local magnetization are not strictly parallel in the connection regions between the straight segments and the corner areas because of the competition between the nonuniform interaction and the anisotropic energy.

At $\mathbf{H}_{ex}=0$ the difference of G between the parallel and perpendicular cases is mostly caused by the domain walls, as **m** is generally parallel to the easy axes of the segments in both cases. For the parallel case, the whole structure can be approximated as a single domain, and the deviation from this structure only causes a small correction. For the perpendicular case, the Néel walls are formed in the corners, pinned at the lines separating regions with different magnetic anisotropy direction. The difference in G between two cases at zero external field demonstrates that DW's contribute a positive MR for the adopted parameters. In the parallel case, with J/Ka^2 decreased the relative direction between the charge moving and the magnetization is only slightly changed, leading to a small negative variation in the conductance. However, in the perpendicular case, a remarkable increase in the conductance appears with the DW thickness decreased (see Fig. 5).

The DW contribution to the MR is due to the rapid variation of the magnetization in the DW regions. This influences the spin-flip scattering of the charge carriers and admixes their spin states,[6,11] leading to the positive MR as discussed

above. DW's can also mix states of different channels via the electronic scattering.[21] For a given energy there are several channels with different longitudinal wave lengths $\lambda_\alpha = 1/k_\alpha$, only those channels with λ_α smaller than or comparable with the DW thickness can be effectively scattered. Consequently, the DW contribution to the MR is remarkably affected by their thicknesses. When the DW thicknesses are reduced, the conductance G of the multidomain structure is increased, since the number of channels which are strongly scattered by DW's is reduced. In Fig. 5 we plot the conductance as a function of J/Ka^2 for both the parallel and perpendicular cases. With the thicknesses diminished, the DW contribution to the MR undergoes a positive to negative transition. At $J_c/K_c a^2 \sim 14$, the conductance curves of the parallel and perpendicular cases intersect. Changing K or, in other word, the fraction of the anisotropic and magnetostatic energies in the free energy, only slightly shifts this crossing point, because in the range of the adopted parameters the variation of the fraction of anisotropic and magnetostatic energies is not important. At the same time, the scattering at the interfaces between the magnetic structure and the nonmagnetic leads can also mix states of different channels, but the principal part of its contribution to the MR is identical for the parallel and perpendicular cases.

In the experiment on the cobalt zigzag wire,[10] the wire width is 250 nm, the DW thickness is 15 nm and their ratio is 0.06. In our theoretical calculation, the wire width is $L_w a = 20a$, whereas the DW thickness at the transition point is $\sqrt{(J_c/K_c)}a \sim 3.7a$ and their ratio is 0.185. Consequently, the zigzag wire in Ref. 10 corresponds to the situation where DW's have ''small'' thicknesses and should contribute a negative MR. This is just the fact shown by the experiment. Thus, the results of our theoretical calculation is qualitatively consistent with the experimental data. In the above calculation, we only study the influence of the spatial variation of the magnetization and do not consider the effect of other types of disorder. To test whether the above results can be obtained from the disordered zigzag wires, we carry out a calculation with disordered site energy introduced in the Hamiltonian (7). Such a calculation can give some insight on the change of behavior of the MR due to the disorder. It is found that the disorder reduces the conductance considerably, but the existence of the transition from the positive to negative MR is robust, and the introduction of disorder can only change the critical point. Our preliminary treatment of the disorder shows that the disorder increases the critical ratio for this transition. So the basic conclusion obtained from the comparison between our theoretical calculation and the experimental results is not changed by the introduction of disorder. The inclusion of another one or two layers in the vertical direction and the inclusion of the influence of $\mathbf{H}_{\rm ex}$ and $\mathbf{H}_{\rm in}$ in Eq. (7) can only cause a small correction in the critical ratio.

From this picture we can explain the previous seemingly contradictory experimental results in a unified manner. What is important in the experiments is the position of the transition from the positive contribution of the DW's for the MR to the negative contribution. This transition is specified by a critical ratio of the DW thickness to a characteristic length, which is the wire width in our case. The critical ratio depends on the parameters of the structure, such as the magnetic configuration, the Fermi energy, etc. Since these parameters are different for various systems, the critical ratio for structures used in various experiments is also different. This leads to the seemingly contradictory phenomenon that DW's can produce either a positive or a negative contribution to the MR.

IV. CONCLUSIONS

We investigate the influence of the domain wall scattering on the magnetoresistance in a planar zigzag structure with the width of the wire much larger than the thickness. We suppose that the easy axis for the magnetization is lying in the zigzag plane. At first we numerically calculate the domain patterns by seeking the location of minima of the total free energy. From this we calculate the conductance of the structure by the combination of the Landauer-Büttiker formula and the transfer matrix method where the obtained magnetization provides an effective field for the motion of the conduction carriers. The calculated results shows that the remanent domain structure relies on the magnetization history. It is a single or multidomain pattern depending on whether the system is firstly magnetized to saturation with the in-plane external field parallel or perpendicular to the zigzag direction. This feature allows us to distinguish the DW contribution to the MR from those due to the other origins. We find that the wide DW's can produce positive contribution to the MR, but with their thicknesses decreased a transition from the positive to the negative contribution occurs. This behavior is due to a type of scattering by the DW's that has not been discussed previously: the mixture of channels with different longitudinal wave vectors. The intensity of this mixture depends on the longitudinal wave lengths of the channels. With the DW thicknesses decreased, the number of channels which is effectively scattered by DW's is also decreased, leading to the positive to negative transition for the DW contribution.

The DW thickness in the experiment[10] falls into the range where DW's should contribute a negative MR, which is consistent with the observed results. What is important in experiments is the position of the transition point because it determines whether a ferromagnetic structure has a positive or a negative MR. The position of the critical point is different in various ferromagnetic structures, leading to different types of the MR behavior. From this picture the previous contradictory experimental results can be explained in a unified manner. The occurrence of the transition is robust to the introduction of other types of disorder. The disorder can vary the position of the transition, but this can not qualitatively alter the basic conclusion from our theoretical calculation.

ACKNOWLEDGMENTS

The author Z.-Y. Zhang acknowledges the support by National Foundation of Natural Science in China Grant No. 10204012, and by the special funds for Major State Basic Research Project No. G001CB3095 of China. S.-J. Xiong acknowledges the support by National Foundation of Natural Science in China Grant No. 10074029, and by the China State Key Projects of Basic Research (Grant No. G1999064509).

*Electronic address: zyzhang@nju.edu.cn
†Electronic address: sjxiong@nju.edu.cn

[1] G. Prinz, Science **282**, 1660 (1998).
[2] I. A. Champbell and A. Fert, in *Ferromagnetic Materials*, edited by E. P. Wohlfarth (North-Holland, Amsterdam, 1982), Vol. 3.
[3] L. D. Landau and E. M. Lifshitz, *Electrodynamics of Continuous Media*, 2nd ed. (Pergamon Press, Headington Hill Hall, England, 1984).
[4] V. Korenman, J. L. Murray, and R. P. Prange, Phys. Rev. B **16**, 4032 (1977).
[5] K. Hong and N. Giordano, J. Magn. Magn. Mater. **151**, 396 (1995); Phys. Rev. B **51**, 9855 (1995).
[6] J. F. Gregg, W. Allen, K. Ounadiela, M. Viret, M. Hehn, S. M. Thompson, and J. M. D. Coey, Phys. Rev. Lett. **77**, 1580 (1996).
[7] S. N. Gordeev, J.-M. L. Beaujour, G. L. Bowden, B. D. Rainford, P. A. J. de Groot, R. C. C. Ward, M. R. Wells, and A. G. M. Jansen, Phys. Rev. Lett. **87**, 186808 (2001).
[8] R. Danneau, P. Warin, J. P. Attane, I. Petej, C. Beigne, C. Fermon, O. Klein, A. Marty, F. Ott, Y. Samson, and M. Viret, Phys. Rev. Lett. **88**, 157201 (2002).
[9] U. Ruediger, J. Yu, A. D. Kent, and S. S. P. Parkin, Appl. Phys. Lett. **73**, 1298 (1998); U. Ruediger, J. Yu, S. Zhang, A. D. Kent, and S. S. P. Parkin, Phys. Rev. Lett. **80**, 5639 (1998).
[10] T. Taniyama, I. Nakatani, T. Namikawa, and Y. Yamazaki, Phys. Rev. Lett. **82**, 2780 (1999).
[11] P. M. Levy and S. Zhang, Phys. Rev. Lett. **79**, 5110 (1997).
[12] G. Tatara and H. Fukuyama, Phys. Rev. Lett. **78**, 3773 (1997).
[13] R. P. van Gorkom, A. Brataas, and G. E. W. Bauer, Phys. Rev. Lett. **83**, 4401 (1999).
[14] D. C. Mattis, *Theory of Magnetism* (Harper & Row, New York, 1965).
[15] A. G. Gurevich and G. A. Melkov, *Magnetization Oscillation and Waves* (CRC Press, Boca Raton, FL, 1996).
[16] G. Tatara and H. Fukuyama, Phys. Rev. Lett. **72**, 772 (1994).
[17] M. Büttiker, Y. Imry, R. Landauer, and S. Pinhas, Phys. Rev. B **31**, 6207 (1985).
[18] For a recent review article, the readers are refered to B. Kramer and A. MacKinnon, Rep. Prog. Phys. **56**, 1469 (1993).
[19] L. Berger, J. Appl. Phys. **55**, 1954 (1984); C.-Y. Hung and L. Berger, *ibid.* **63**, 4276 (1988); A. K. Agarwala and L. Berger, IEEE Trans. Magn. **MAG-22**, 544 (1986).
[20] J. Smit, Physica (Amsterdam) **16**, 612 (1951); T. R. McGuire and R. I. Potter, IEEE Trans. Magn. **MAG-11**, 1018 (1975); R. I. Potter, Phys. Rev. B **10**, 4626 (1974).
[21] G. G. Cabrera and L. M. Falicov, Phys. Status Solidi **61**, 539 (1974); **62**, 217 (1974).